International Journal of
Agriculture, Environment and Food Sciences
e-ISSN: 2618-5946 https://dergipark.org.tr/jaefs

DOI: https://doi.org/10.31015/2025.2.8 Int. J. Agric. Environ. Food Sci. 2025; 9 (2): 331-347

Sensitivity analysis of uranium reduction and its reoxidation by Fe(III)-(hydr)oxides biogeochemical reaction dynamics

Sema Sevinç Şengör[1]

[1]Middle East Technical University, Engineering Faculty, Environmental Engineering Department, Ankara, Turkey

Article History
Received: January 9, 2025
Accepted: May 12, 2025
Published Online: June 17, 2025
Revised: June 29, 2025

Article Info
Type: Research Article
Subject: Environmental Assessment and Monitoring

Corresponding Author
Sema Sevinç Şengör
ssengor@metu.edu.tr

Author ORCID
[1]https://orcid.org/0000-0003-3944-1172

Available at
https://dergipark.org.tr/jaefs/issue/91914/1616762

DergiPark AKADEMİK

Abstract

Sensitivity analysis is a useful tool in modeling environmental systems to identify how variations in model parameters would impact model outputs. In modeling environmental processes in biological systems, the rates and processes of biodegradation reactions are described using biokinetic parameters. Reducing the parameter uncertainty in modeling efforts would be important for reliable and accurate model results. Understanding the impact of variations in the biokinetic parameters would be highly critical to help to reduce the uncertainity in model predictions. This study presents a sensitivity analysis of the biokinetic parameters affecting the biogeochemical reaction network for uranium biotransformation dynamics. The main reactions included in the network are sulfate bioreduction, Fe(III) bioreduction, U(VI) reduction to U(IV), Fe(III) reduction by sulfide, U(IV) reoxidation to U(VI) and sulfur precipitation-dissolution reactions. The sensitivity analysis results revealed that changes in the biokinetic parameters to the sulfate bioreduction reaction had the most significant impact to the model outputs. Among the parameters, maximum substrate utilization rate and yield coefficient had the most significant impact, whereas half-saturation constants had slightly less impact on model results. U(VI) concentration predictions were the most sensitive towards variations in biokinetics parameters among the species monitored within the biogeochemical reaction network. Fe(III) bioreduction, Fe(III) reduction by sulfide and sulfur precipitation/dissolution reactions were not shown to be sensitive to any changes in the biokinetic parameters.

Keywords: Sensitivity analysis, Biokinetic parameters, Uranium, Reoxidation, Biogeochemical processes

Cite this article as: Sengor, S.S. (2025). Sensitivity analysis of uranium reduction and its reoxidation by Fe(III)- (hydr)oxides biogeochemical reaction dynamics. International Journal of Agriculture, Environment and Food Sciences, 9 (2): 331-347. https://doi.org/10.31015/2025.2.8

INTRODUCTION

Modeling and simulations are important components of biodegradation processes in terms of efficient process design and evaluation of system performance. Simulations of contaminant biodegradation processes can be used both to understand the system dynamics as well as to predict contaminant concentrations under different environmental factors that would affect the operational performance. Due to the complex nature of the environmental systems and variability in environmental conditions which might change over space and time, some level of uncertainty might be introduced into the models. Depending on the choice of the model structure, uncertainty in the model parameters would need to be considered for accurate predictions and overall reliability of the model outcomes. The parameters used in the models developed for the biotreatment processes are commonly referred to as biokinetic parameters, which are constants used to describe the rates and processes of the biological degradation reaction of concern. An accurate and reliable estimation of these biokinetic parameters are highly important for accurate and reliable simulation results that can efficiently represent the system (Zhou et al., 2012).

Sensitivity analysis is a useful tool to investigate the uncertainty of biokinetic parameters in model predictions and also determine which parameter would have the most significant impact on the model outputs (Neumann 2012). Various studies have been conducted to investigate the effect of kinetic parameters in modeling a diverse range of pollutant degradation processes by means of sensitivity analysis (Seyfi et al., 2021; Baalbaki et al., 2017; Vázquez-Rodríguez et al., 2006; Lin and Wu 2011; Malaguerra et al., 2011; China and Kumar, 2004; Pontes et al.,

2010). However, studies related to sensitivity analysis for biological transformations of uranium in environmental systems are highly limited.

Uranium has been one of the most important contaminants that has been reported in water, soil and sediments; and has been considered to be a significant threat due to its mobility, solubility and toxicity (Renshaw et al., 2005; Tokunaga et al., 2008; Wilkins et al., 2006). The oxidized form of U(VI), which is commonly found as the uranyl ion (OU_2^{+2}) is more toxic, soluble and mobile; and can be microbially reduced to the tetravalent form, U(IV), which is less toxic, less mobile and insoluble in the form of biogenic uraninite mineral ($UO_2(s)$) under reducing conditions (Gu et al., 2005; Renshaw et al., 2005; Wufuer et al., 2017). This microbially mediated remediation strategy for soluble U(VI) to insoluble U(IV) has therefore been considered to be the most cost-effective and promising approach among other removal mechanisms for uranium. Metal-reducing bacteria, particularly iron reducing and sulfate-reducing bacteria (SRB) can facilitate the reduction of U(VI) to U(IV) in the presence of suitable electron donors (Anderson et al., 2003; Gihring et al., 2011; Wufuer et al., 2017; Yabusaki et al., 2011). However, experiments conducted by Sani et al. (2004) reported that the insoluble uraninite might be reoxidized back to the soluble U(VI) in the presence of Fe(III)-hydr(oxides) when the electron donor in the medium (e.g., lactate) is consumed, highlighting the challenge for uranium bioremediation efforts. Spycher et al. (2011) have described the biogeochemical reaction network of the experiments conducted by Sani et al. (2004) capturing the important thermodynamic constraints effecting the uranium transformations. In their study, the competing rates of reactions for U(IV) reoxidation, Fe(II) and sulfide generation were presented and biokinetic parameters for the biogeochemical reactions were calibrated to capture the experiment data. Particular emphasis has been provided for the relative rates of U(IV) reoxidation versus Fe(III) oxidation by sulfide, where sulfide is generated by sulfate reduction reactions in the system. Based on the sensitivity of the competing reaction systems, it would be important to investigate the impact of uncertainty of the calibrated biokinetic parameters on model outcomes, as the variations in these parameters would reflect the local changes in the factors affecting the relative rates of the reactions. Variations on the calibrated biokinetic parameters would be highly likely in natural systems, which would have significant influence on contaminant predictions, especially for similar biogeochemical reaction networks consisting of a delicate balance between competing reactions. Although Spycher et al. (2011) have described the biogeochemical reaction network, the sensitivity of the biokinetic parameters on model outcomes related to uranium transformations has not been examined before. Therefore, the present study provides a sensitivity analysis of the biokinetic parameters affecting the biogeochemical reaction network dynamics. The extent of the effect of each parameter on the overall biogeochemical processes and competing reactions are demonstrated here.

MATERIALS AND METHODS

Description of the Biogeochemical Reaction Network

The biogeochemical reaction network is composed of the biotic and abiotic reactions outlined by Spycher et al. (2011), which include sulfate bioreduction, Fe(III) bioreduction, U(VI) reduction, Fe(III) reduction by HS^-, U(IV) reoxidation and sulfur precipitation-dissolution reactions as described in detail below.

Sulfate bioreduction: microbial reduction of sulfate to HS^-, where lactate is oxidized to acetate is expressed as follows:

$$2C_3H_5O_3^- + SO_4^{-2} \rightarrow 2CH_3COO^- + 2CO_3^{-2} + HS^- + 3H^+ \quad (1)$$

Fe(III) bioreduction: microbial reduction of Fe(III) to Fe^{+2} coupled to lactate oxidation to acetate is expressed as follows:

$$C_3H_5O_3^- + 4Fe^{+3} + 2H_2O \rightarrow CH_3COO^- + CO_3^{-2} + 4Fe^{+2} + 6H^+ \quad (2)$$

These microbially-mediated reactions are modeled using dual-Monod biomass growth kinetics, where the reaction rate, R is described as (Spycher et al., 2011; Şengör et al., 2015):

$$R = qC_B \frac{C_D}{k_D + C_D} \frac{C_A}{k_A + C_A} f_G \quad (3)$$

with

$$R_{rxn} = YR - bC_B \quad (4)$$

$$f_G = (1 - Q/K) \quad (5)$$

where C_B, C_D, and C_A, are the concentrations of biomass, electron donor and electron acceptor, respectively (in units of moles/L). k_D and k_A are the half saturation constants for electron donor and acceptor, respectively (in units of moles/L). q is the rate of maximum substrate utilization (in units of moles per time, per biomass), Y is the microbial yield coefficient (in units of biomass per substrate), b is the cell decay rate (in units of per time). f_G is the term for affinity which indicates whether the reaction is at equilibrium (being equal to 0) or away from equilibrium (being equal to 1), where Q is the ion activity product and K is the equilibrium constant of the corresponding reaction. For the Fe(III) bioreduction reaction, the rate is considered to be only limited by the

electron donor, lactate, as unlimited supply of the electron acceptor, (Fe(III) or hematite solids) are assumed; therefore, the Monod term consisting of $C_A/(k_A+C_A)$ in Eqn. (3) is taken to be equal to 1 (Spycher et al., 2011).

U(VI) reduction: The combined biotic and abiotic U(VI) reduction reaction to U^{+4} is expressed as follows:

$$4UO_2^{+2} + HS^- + 7H^+ \rightarrow 4U^{+4} + SO_4^{-2} + 4H_2O \quad (6)$$

The rate of this reaction was limited by lactate, as expressed by the following Monod kinetics:

$$R = r\frac{C_D}{k_D + C_D} f_G \quad (7)$$

where r and k_D are the reaction rate constant (in units of mol/time) and half saturation constant for lactate (in units of moles/L), respectively, and these parameters were adjusted to reproduce the observed experimental results by Sani et al. (2004). As discussed by Spycher et al. (2011), implicitly limiting this reaction by lactate was the simplest approach tested while also the number of adjustable model parameters were minimized.

Fe(III) reduction by HS^-: The fully abiotic Fe(III) reduction to Fe^{+2} reaction coupled by HS^- oxidation to sulfate is describes as:

$$8Fe^{+3} + HS^- + 4H_2O \rightarrow 8Fe^{+2} + SO_4^{-2} + 9H^+ \quad (8)$$

U(IV) reoxidation: The fully abiotic U(IV) oxidation to U(VI) coupled to Fe(III) reduction to Fe^{+2} reaction is describes as:

$$U^{+4} + 2Fe^{+3} + 2H_2O \rightarrow UO_2^{+2} + 2Fe^{+2} + 4H^+ \quad (9)$$

Sulfur precipitation/dissolution: The fully abiotic Sulfur precipitation/dissolution reaction is also expressed kinetically to yield consistent results with experimental data, and expressed as:

$$2Fe^{+3} + HS^- \rightarrow 2Fe^{+2} + S_{(s)} + H^+ \quad (10)$$

The rates of the abiotic reactions were considered to be limited only by thermodynamic constraints and therefore expressed as:

$$R = r f_G \quad (11)$$

where r (in units of moles per time) is the reaction rate constant.

The reaction rate parameters discussed above were calibrated by fitting the predicted concentrations of lactate, acetate, sulfate and U(VI) with the measured experimental data, where the calibrated parameters are provided in Table 1, as reported by Spycher et al. (2011).

An illustration of the conceptual framework of biogeochemical reactions is provided in Figure 1. Sulfate bioreduction reaction to biogenic HS^- and the Fe(III) bioreduction reaction to Fe^{+2}, coupled to the oxidation of lactate, providing the electrons from the organic substrate source, are illustrated on the left-hand-side of the Figure. The abiotic Fe(III) reduction by the available HS^- producing Fe^{+2} and sulfate; as well as the abiotic sulfur precipitation/dissolution reaction oxidizing the available HS^- to produce sulfur minerals as $S_{(s)}$ are also depicted. Right-hand-side of the Figure shows the U(VI) reduction, where aqueous U(VI) is reduced to U(IV) minerals; as well as the reoxidation of U(IV) back to soluble U(VI) into the medium.

Sensitivity Analysis

Sensitivity analysis relies on a robust statistical analysis, which provides the essential tools for quantifying the variability and uncertainty in model parameters. Sensitivity analysis to quantify the impact of each variable on the simulation results has been conducted using the least-square method, where the value of each variable is increased and decreased by 50 % one at a time from the baseline value, while keeping the other parameters constant. The least-square method is a commonly used statistical approach to minimize the sum of the squares of the differences between baseline and simulated values. The baseline values are the previously calibrated model parameters as described by Spycher et al. (2011) for the concentration data obtained for sulfate, lactate, acetate and U(VI) with regards to the U(VI) bioreduction followed by U(IV) reoxidation batch experiments originally conducted by Sani et al. (2004). The least-square value (LSV) which provides a quantitative comparison of simulated and baseline simulation results is described as (Lin and Wu, 2011):

$$\mathrm{LSV} = \frac{1}{N}\sum_{i=1}^{N}\sqrt{\frac{\left(S_{simulated,i} - S_{baseline,i}\right)^2}{\left(S_{baseline,i}\right)^2}} \quad (12)$$

where N refers to the number simulation data points, $S_{simulated,i}$ and $S_{baseline,i}$ are the simulation and baseline simulation points, respectively. In the least-square method, a decrease in the LSV results indicates a strong agreement between the model simulation and baseline simulation results (Lin and Wu, 2011).

In order to quantify the model simulation results with the measured experimental data points, two statistical parameters are used: coefficient of determination, R2, and Mean Relative Error (MRE). Coefficient of determination, R2 can be expressed as (Walpole & Myers, 1989):

$$R2 = 1-\left\{\frac{\sum(X-Ssimulated,i)^2}{[\sum X^2]-\frac{[\sum X]^2}{N_{data}}}\right\} \quad (13)$$

Mean Relative Error (MRE) can be described as (Scarlat et al., 2014):

$$MRE = \frac{1}{N_{data}}\sum_{i=1}^{N_{data}}\frac{|S_{simulated,i}-X_i|}{X_i} \quad (14)$$

where N_{data} is the number of experimental data points, X is the experimental data and $S_{simulated,I}$ is the simulation data points. Ideally, the R2 value of a perfectly fitted model should be close to 1 and the residual errors should be close to zero, where MRE would approach zero (Moriasi et al., 2015).

The simulations presented in this study are carried out by the speciation and geochemical calculation program code PHREEQC (Parkhurst and Appelo, 2013). PHREEQC is a widely used computer program that is designed to perform a wide variety of aqueous geochemical calculations. The program implements various geochemical speciation reactions including batch-reactions, one-dimensional transport, and inverse geochemical calculations with reversible and irreversible reactions (Parkhurst and Appelo, 2013).

Table 1. Kinetic rate expresions and calibrated parameters for the U(VI) bioreduction reaction network (from Spycher et al., 2011)

Reaction	**Kinetic Rate Expresssion**	**Calibrated Parameters Considered as Baseline Values**				
		q (mol/s/mg$_{cells}$) or r (mol/s)	**k_D (mol/L)**	**k_A (mol/L)**	**Y (mg$_{cells}$/mol)**	**b (1/s)**
Sulfate bioreduction	$R = qC_B \frac{C_D}{k_D + C_D}\frac{C_A}{k_A + C_A} f_G$	10^{-8}	$2x10^{-2}$	$2x10^{-2}$	1600	10^{-8}
Fe(III) bioreduction	$R = qC_B \frac{C_D}{k_D + C_D}\frac{C_A}{k_A + C_A} f_G$	10^{-11}	$2x10^{-2}$	-	1600	10^{-8}
U(VI) reduction	$R = r\frac{C_D}{k_D + C_D} f_G$	$8x10^{-11}$	$4x10^{-2}$			
Fe(III) reduction by HS-	$R = r f_G$	$0.45x10^{-11}$				
U(IV) reoxidation	$R = r f_G$	$2x10^{-11}$				
Sulfur ppt/ dissolution	$R = r f_G$	$1.4x10^{-11}$				

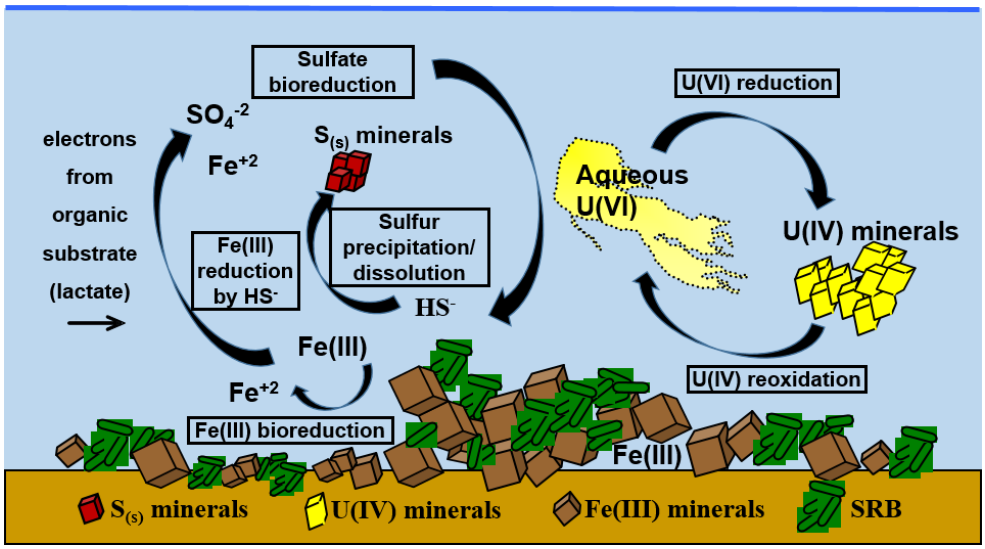

Figure 1. Illustration of the conceptual framework for biogeochemical reactions

RESULTS AND DISCUSSION

In this section, the results of the sensitivity analysis are presented along with the details of the impact of each biokinetic parameter on each of the biogeochemical reactions: sulfate bioreduction, Fe(III) bioreduction, U(VI) reduction, Fe(III) reduction by HS-, U(IV) reoxidation and Sulfur precipitation/dissolution reactions. The sensitivity analysis is conducted where the value of the selected parameter is varied ± 50% while all other parameters remained constant at base-line values, as reported in Table 2. Table 2a presents the results of average LSV of each biokinetic parameter variation by 50% increase on U(VI) concentration, acetate concentration and sulfate concentration predictions; and Table 2b presents the results of average LSV variation by 50% decrease on the concentration predictions. The impact of ± 50% biokinetic parameter variations on the discrepancies of model results with the measured data is also demonstrated with R2 and Mean Relative Error Analysis results for each reaction, as seen in Table 2a and 2b. The biokinetic parameters tested in this study include maximum substrate utilization rate (q), half saturation constant for electron donor (k_D) and acceptor (k_A) for sulfate bioreduction reaction; maximum substrate utilization rate (q) and half saturation constant for electron donor (k_D) for Fe(III) bioreduction reaction; microbial yield coefficient (Y) and cell decay rate coefficient (b) for sulfate bioreduction & Fe(III) bioreduction reactions; rate constant (r) for U(VI) reduction reaction; rate constant (r) for Fe(III) reduction by HS^- reaction; rate constant (r) for U(IV) reoxidation reaction and rate constant (r) for Sulfur precipitation/dissolution reaction. The results for each reaction is discussed in detail below.

Sulfate bioreduction

Figure 2 shows the impact of maximum substrate utilization rate (q) on (a) sulfate, (b) acetate, (c) U(VI) concentration; impact of half saturation constant for electron donor (k_D) on (d) sulfate, (e) acetate, (f) U(VI) concentration; and the impact of half saturation constant for electron acceptor (k_A) on (g) sulfate, (h) acetate, (i) U(VI) concentration with regards to the sulfate bioreduction reaction. As seen from Figure 2 (a-e) and Table 2, a 50 % increase in the maximum substrate utilization rate (q) has a slight decreasing effect in sulfate concentrations and corresponding slight increasing effect in acetate concentrations with average LSV of 0.0483 and 0.0792, respectively; following the reaction kinetics as shown in Eqn (3) and the stoichiometry of reaction (1). A 50 % decrease in q, however, results in a more significant increase in sulfate and decrease in acetate concentrations with LSV of 0.2358 and 0.1648, respectively. The U(VI) concentration predictions are more significantly affected as can be seen from Figure 2c and higher average LSV values, especially with 0.6459 LSV for 50% decrease in q is observed. As seen from the reaction (1), when sulfate reduction reaction is increased, this causes a further decrease in lactate concentrations, which affects the rate of U(VI) reduction reaction, where the rate of this reaction is limited by lactate as by Eqn (7). The decreased lactate in the system results in a decrease in U(VI) reduction reaction with higher U(VI) concentrations; and reverse effects are observed with the decrease in sulfate reduction reaction, resulting in U(VI) concentration trends as depicted in Figure 2c.

50 % increase and decrease in the half saturation constant for electron donor (k_D) and acceptor (k_A) has slight impact on sulfate and acetate concentration trends as can be seen from Figure 2d & 1e, and Figure 2g & 1h, respectively, as well as from the relatively lower LSV results (ranging from 0.0475-0.0706) as seen in Table 2. An increase in either k_D or k_A values results in a decrease in the overall rate of sulfate reduction reaction as seen in Eqn. (3) which ends up with higher sulfate and lower acetate concentrations based on reaction (1). This has relatively more significant impact again on the U(VI) concentrations, as can be seen from Figure 2(f) and 2(i) and

relatively higher LSV results (ranging from 0.3243-0.3879) in Table 2. Again, based on the available lactate in the environment, a decrease in the overall rate of sulfate reduction reaction results in higher lactate availability, which causes an increase in the U(VI) reduction reaction (Reaction 6) ending up in lower U(VI) (and again with the reverse effect resulting in higher U(VI)) concentrations, as seen in Figures 2(f) and 2(i).

The comparison of model predictions with the measured data is also assessed by R2 and MRE values for uranium, acetate and sulfate concentrations, as can be seen from Table 2. As can be seen from the analysis results, an increase in the sulfate bioreduction reaction by either 50% increase in q or decrease in k_D or k_A values results in a further improved fit for sulfate and acetate concentrations, as seen from Figure 2 comparative simulation runs with the measured data points. This can also be confirmed with high R2 values (ranging from 0.9788-0.9854) and very low MRE values (ranging from 0.0313-0.1299) as seen in Table 2, indicating a very good fit between measured and predicted values for sulfate and acetate. However, this increase in the sulfate bioreduction reaction did not improve the fits for U(VI) concentrations, confirmed with relatively lower R2 and MRE values as seen in Table 2. When the sulfate bioreduction reaction rate is decreased on the other hand, either by 50% decrease in q or increase in k_D or k_A values, deviations from the measured data are observed for all concentration predictions, including sulfate, acetate and U(VI), as can be seen from Figure 2 and statistical analysis results in Table 2 (relatively lower R2 values ranging from 0.6414-0.9429, relatively higher MRE values ranging from 0.1378-0.5163) as seen from Table 2.

Sulfate bioreduction reaction has important environmental implications, where it can be used to treat sulfate-rich wastewaters, which can come from various industrial sources. With the production of biogenic sulfide, HS^- becomes available to be used in the proceeding chain of reactions to reduce Fe(III) and/or U(VI) in the reducing environment. The sulfides can also precipitate to remove other heavy metals, such as copper, zinc, cadmium, lead, nickel if present in the medium. These metal sulfides are insoluble and can be recovered for reuse purposes (Lens et al., 2008).

Fe(III) bioreduction

Figure 3 shows the impact of maximum substrate utilization rate (q) on (a) sulfate, (b) acetate, (c) U(VI) concentration; and the impact of half saturation constant for electron donor (k_D) on (d) sulfate, (e) acetate, (f) U(VI) concentration with regards to the Fe(III) bioreduction reaction. As seen from Figure 3 and relatively very low average LSV results (ranging between 0.0002-0.0037) in Table 2, the sulfate, acetate and U(VI) concentrations do not result in any significant deviations when the biokinetic parameters for Fe(III) bioreduction reaction is varied ±50 % from the baseline value. The lack of sensitivity of the q and k_D parameters revealed that the Fe(III) bioreduction reaction did not have much controlling factor among the biogeochemical reaction network. Model prediction comparisons with the measured data are therefore ultimately aligned with the baseline simulation outcomes, where a reasonably good fit of the original model predictions can be seen from the R2 (ranging between 0.9537-0.9721) and MRE (ranging between 0.0911-0.2330) values for uranium, acetate and sulfate concentrations as seen in Table 2.

The impact of microbial yield coefficient (Y) on (a) sulfate, (b) acetate, (c) U(VI) concentration; and the impact of cell decay rate coefficient (b) on (d) sulfate, (e) acetate, (f) U(VI) concentration for the sulfate bioreduction & Fe(III) bioreduction reactions are shown in Figure 4. The microbially mediated sulfate bioreduction and Fe(III) bioreduction reactions share the common growth kinetic parameters of Y and b, as seen from Eqn. (4). As seen from Figure 4(a-c) and Table 2 sensitivity analysis results, the ±50 % variation of Y from the baseline value results in a similar sensitivity in sulfate, acetate and U(VI) concentrations, compared to the effect with ±50 % variation in q for sulfate bioreduction (see Figure 2(a-c)), where 50% reduction in Y had again slightly more impact. Based on the reaction rates modeled with dual-Monod biomass growth kinetics (Eqn. 3), the similar impact of Y and q on the reaction rates would be expected. On the other hand, ±50 % variation of cell decay rate coefficient (b) did not have any significant deviations on the sulfate, acetate and U(VI) concentrations, indicating that cell decay rate coefficient was not sensitive on the microbially-mediated reaction network considered in the system (see Figures 4(d-f)). The comparison of model predictions with the measured data can be seen in Table 2 by means of the R2 and MRE values for uranium, acetate and sulfate concentrations pertaining to the variations in Y and b parameters.

This reaction has important implications from environmental perspective, where the reduction of Fe(III) to Fe(II) can degrade organic contaminants. The produced Fe(II) can participate in other redox reactions, potentially reducing other contaminants. The reaction can also lead to the formation of reactive minerals such as magnetite (Fe_3O_4) and green rust, where these minerals can adsorb and degrade contaminants, providing a long-term remediation solution (Chaudhuri et al., 2001).

U(VI) reduction

The impact of rate constant (r) on (a) sulfate, (b) acetate, (c) U(VI) concentration; and the impact of half saturation constant for electron donor (k_D) on (d) sulfate, (e) acetate, (f) U(VI) concentration for the U(VI) reduction reaction is provided in Figure 5. As can be seen from Figure 5(a-b) and Figure 5(d-e), sulfate and acetate concentration predictions are not sensitive to the variations in either r or k_D. However, U(VI) concentrations

resulted in significant deviations from the baseline outcome results, when the biokinetic parameters, r or k_D, are varied ±50%. The resulting sensitivity analysis can be seen from the relatively higher LSV results in Table 2, ranging between 0.3470-0.5982. As seen from Reaction (6), when the rate of U(VI) reduction reaction is increased either by an increase in the rate constant, r, or a decrease in the half saturation constant, k_D, further depletion in U(VI) results in the decrease of U(VI) concentrations, as expected from the reaction stoichiometry. Similarly, the reverse effect is seen when the rate is decreased by decreasing the rate constant, r, or increasing the half saturation constant, k_D. Significant deviations from the measured data points for U(VI) concentration trends can also be seen from the R2 (ranging between 0.6788-0.8533) and MRE (ranging between 0.4162-0.6682) values in Table 2. The greater sensitivity of U(VI) might be attributed to the relatively lower concentration values compared to sulfate and acetate, where variations in lower concentration amounts might show more visible effect in general.

U(VI) reduction reaction is the main reaction mediating the conversion of aqueous U(VI) into insoluble U(IV) form; which is considered as a promising strategy for in-situ remediation of subsurface uranium. This reaction has significant environmental implications, where the engineered biostimulation of indigenous microorganisms to mediate the conversion of U(VI) to immobile U(IV) form has been demonstrated in various uranium contaminated sites (Anderson et al., 2003; Yabusaki et al., 2011).

Fe(III) reduction by HS^- reaction

Figure 6 shows the impact of rate constant (r) on (a) sulfate, (b) acetate, (c) U(VI) concentration for the Fe(III) reduction by HS^- reaction. As can be seen from Figure 6, sulfate, acetate and U(VI) concentration trends did not result in any significant deviations when the rate of Fe(III) reduction by HS^- is varied ±50 % from the baseline value. The relatively low average LSV results, ranging between 7.55E-6-0.0191, can also be seen in Table 2. The lack of sensitivity of the rate constant, r, on concentration prediction outcomes demonstrated that the Fe(III) reduction by HS^- reaction did not have much influence over the biogeochemical reaction network considered in this study.

Similar to the Fe(III) bioreduction, Fe(III) reduction by HS^- reaction has impacts on water quality based on the release of soluble Fe(II) into the subsurface pore water environment, which can enhance the mobility and bioavailability of iron in solution. This would facilitate the transport of iron and other nutrients, supporting microbial activity and bioremediation processes. Again, the formation of magnetite and/or green rust as secondary reactive minerals can also take place, which can also serve as adsorbents for removing various pollutants in the media (Chaudhuri et al., 2001).

U(IV) reoxidation

The impact of rate constant (r) on (a) sulfate, (b) acetate, (c) U(VI) concentration for the U(IV) reoxidation reaction is depicted in Figure 7. As seen from Figure 7, the results of the sensitivity analysis show the sensitivity of U(VI) concentration predictions to the ±50% variations in r. The relatively higher LSV results for U(VI) ranging between 0.2569-0.3282 can also be seen in Table 2. When the rate of U(IV) reoxidation reaction (see Reaction 9) is increased by increasing the rate constant, r, further increase in U(VI) results based on the reaction stoichiometry; and the reverse effect causes a decrease in the U(VI) concentration trends when the rate constant, r, is decreased. The observed deviations from the measured data points for U(VI) can also be seen from the R2 (ranging between 0.8727-0.8854) and MRE (ranging between 0.3242-0.3595) values in Table 2. The sulfate and acetate concentrations on the other hand, were not sensitive to the variations in r, as can also be seen from the relatively low LSV results (ranging between 1.33E-6-3.18E-6) in Table 2. The greater sensitivity of U(VI) results might again be due to the relatively lower concentration values of U(VI), when compared to sulfate and acetate concentrations.

From an environmental point of view, this reaction has significant impact in terms of the stability of bioreduced uranium. U(IV) has been shown to be susceptible to re-oxidation and remobilization under electron-donor limiting and sulfate reducing conditions (Sani et al., 2004). Subsurface porous medium is known to contain Fe(III)-oxide minerals, where the available Fe(III) can serve as the electron acceptor to reoxidize U(IV) back to U(VI), thereby significantly affecting uranium biodegradation efforts (Sani et al., 2004; Spycher et al, 2011).

Sulfur precipitation/dissolution reaction

The impact of rate constant (r) on (a) sulfate, (b) acetate, (c) U(VI) concentration for the sulfur precipitation/dissolution reaction is illustrated in Figure 8. As can be seen from Figure 8, sulfate, acetate and U(VI) concentration trends did not result in any significant fluctuations with the ±50% variations in the sulfur precipitation/dissolution reaction rate constant. The relatively low average LSV results, ranging between 2.4E-7-0.0156, can also be seen in Table 2. The sensitivity analysis results showed that the sulfur precipitation/dissolution reaction rate was also insensitive to the overall concentration predictions, and therefore this reaction did not have much control towards the biogeochemical process dynamics.

Considering the environmental impact of this reaction, sulfur precipitation can influence the pH and redox conditions of the water, which can have further influence on the solubility and mobility of other contaminants in

the medium. Elemental sulfur also plays an important role in biogeochemical cycling of heavy metals, where its dissolution to form hydrogen sulfide, HS-. would facilitate the formation of metal sulfide precipitates to remove metal contaminants from aqueous environment.

Overall Evaluation

The results show that variation in the kinetic parameters pertaining to the sulfate bioreduction reaction had the most influence over the biogeochemical reaction dynamics considered in this study. For sulfate bioreduction, the biokinetic parameters, k_D, and k_A had similar sensitivity towards sulfate and acetate concentration predictions, whereas 50 % decrease in q as well as Y had the most impact. Changes in the biokinetic parameters for U(VI) reduction and U(IV) reoxidation reactions did not show any sensitivity towards the model outcomes, except for U(VI) concentration predictions. Among the concentrations tested, U(VI) concentration was observed to be the most sensitive parameter for the changes in biokinetics parameters among the competing biogeochemical reaction network, which might be due to its lower concentration values compared to other species concentrations in the system. Fe(III) bioreduction reaction kinetic parameters, cell decay rate coefficient, Fe(III) reduction by HS^- and sulfur precipitation/dissolution reaction's kinetic parameters also did not significantly affect the biogeochemical process dynamics.

Sensitivity analysis studies reported in literature have also demonstrated the impact of biokinetic parameters in modeling various contaminant biodegradation processes, highlighting the importance of accurate monitoring and prediction of the specific contaminant of concern. Sensitivity analyses for bioactive granular activated carbon adsorbers for alachlor removal was studied by Badriyha et al. (2003), where their results for thin biofilm model showed the significant sensitivity of the Monod coefficients, maximum substrate utilization rate and Monod half-velocity constant, and moderate sensitivity of maximum biofilm thickness on process performance. Den and Pirbazari (2002) conducted a study to investigate the biokinetic and adsorption parameters for TCE using a series of minibiofilter and miniadsorber column experiments, where model sensitivity was examined to understand the effect of adsorption equilibrium, transport and biological parameters on biofilter dynamics. Sensitivity analysis results indicated that the Monod constants (maximum substrate utilization rate constant and half saturation constant for Monod kinetics) as well as the biofilm thickness had a significant control on the biofilter performance. Sensitivity analysis study conducted by Dastidar and Wang (2009) for biological oxidation of As (III) in batch reactors for various As concentration ranges revealed that their yield coefficient and substrate inhibition coefficient were the most sensitive parameters in their model predictions, whereas endogenous decay coefficient was the least sensitive. In their another fixed-film bioreactor modeling study for biological oxidation of As (III) under different operating conditions, maximum specific utilization rate constant was observed to be the most sensitive parameter under steady-state conditions compared to half-saturation constant (Dastidar and Wang, 2012). A study reported by Zhou et al. (2012), which quantified the growth biokinetic parameters of biofilm in wastewater treatment using oxygen microelectrodes showed that their maximum specific oxygen uptake rate was more sensitive in their Monod kinetic model, compared to their Monod half saturation constant and maintenance decay coefficient for oxygen. The determination of biokinetic parameters of biofilms by measuring oxygen uptake profiles was also investigated by Riefler et al. (1998) for a completely mixed attached growth bioreactor, where their sensitivity analysis demonstrated that their maximum specific growth rate coefficient as well as half-saturation coefficient were the most sensitive parameters in their transient biofilm model.

The results demonstrated in the current study might have important consequences in modeling uranium contaminated environments for U(VI) removal strategies, where similar competing reaction process dynamics would be of concern. The higher sensitivity of U(VI) to changes in biokinetics parameters would imply the importance of sensitivity analysis in this context, as U(VI) might the primary monitored contaminant in the system. Due to the nature of local variabilities in biokinetic parameters especially in the natural environment, uncertainity in the calibrated parameters in modeling efforts is of paramount importance, especially for modeling complex biogechemical reaction networks. Understanding how the variations in the calibrated parameters would affect the model output would help to reduce model uncertainity in model predictions. Also, the sensitivity of biokinetic parameters over a range various competing reactions in the system would provide useful information to understand the system dynamics and behavior under different conditions. Furthermore, sensitivity analysis of model input parameters would help to identify the key parameters that control the system performance, guiding model refinement and improvement in efforts to increase process efficiency and system design.

Table 2a. Sensitivity analysis results of the increased 50 % variation of biokinetic parameters on each reaction.

Reaction	**Parameter**	**Average least-square value**			
	Baseline value	Increased 50 %	Uranium concentration	Acetate concentration	Sulfate concentration
Sulfate bioreduction	q (10^{-8} mol/s/mg_{cells})	$1.5x10^{-8}$	LSV = 0.3628 R2 = 0.8696 MRE=0.3798	LSV = 0.0792 R2 = 0.9824 MRE=0.0313	LSV = 0.0483 R2 = 0.9788 MRE=0.1328
	k_D ($2x10^{-2}$ mol/L)	0.03	LSV = 0.3243 R2 = 0.8762 MRE=0.3472	LSV = 0.0495 R2 = 0.9429 MRE=0.1378	LSV = 0.0570 R2 = 0.9415 MRE=0.2412
	k_A ($2x10^{-2}$ mol/L)	0.03	LSV = 0.3879 R2 = 0.8449 MRE=0.3799	LSV = 0.0604 R2 = 0.9347 MRE=0.1487	LSV = 0.0667 R2 = 0.9317 MRE=0.2567
Fe(III) bioreduction	q (10^{-11} mol/s/mg_{cells})	$1.5x10^{-11}$	LSV = 0.0019 R2 = 0.9541 MRE=0.2318	LSV = 0.0004 R2 = 0.9702 MRE=0.0911	LSV = 0.0037 R2 = 0.9721 MRE=0.1754
	k_D ($2x10^{-2}$ mol/L)	0.03	LSV = 0.0009 R2 = 0.9538 MRE=0.2330	LSV = 0.0002 R2 = 0.9700 MRE=0.0916	LSV = 0.0018 R2 = 0.9717 MRE=0.1779
Sulfate bioreduction & Fe(III) bioreduction	Y (1600 mgc_{ells}/mol)	2400	LSV = 0.1960 R2 = 0.9327 MRE=0.2609	LSV = 0.0303 R2 = 0.9828 MRE=0.0550	LSV = 0.0274 R2 = 0.9840 MRE=0.1325
	b (10^{-8} 1/s)	$1.5x10^{-8}$	LSV = 0.0012 R2 = 0.9539 MRE=0.2329	LSV = 0.0002 R2 = 0.9699 MRE=0.0916	LSV = 0.0002 R2 = 0.9718 MRE=0.1774
U(VI) reduction	r ($8x10^{-11}$ mol/s)	$1.2x10^{-10}$	LSV = 0.4985 R2 = 0.7911 MRE=0.4418	LSV = 2.58E-5 R2 = 0.9700 MRE=0.0915	LSV = 0.0011 R2 = 0.9718 MRE=0.1769
	k_D ($4x10^{-2}$ mol/L)	0.06	LSV = 0.3470 R2 = 0.8533 MRE=0.4162	LSV = 1.38E-5 R2 = 0.9700 MRE=0.0915	LSV = 0.0008 R2 = 0.9719 MRE=0.1774
Fe(III) red. by HS-	r ($0.45x10^{-11}$ mol/s)	$6.75x10^{-12}$	LSV = 0.0150 R2 = 0.9578 MRE=0.2240	LSV = 7.8E-6 R2 = 0.9700 MRE=0.0915	LSV = 0.0010 R2 = 0.9719 MRE=0.1767
U(IV) reoxidation	r ($2x10^{-11}$ mol/s)	$3x10^{-11}$	LSV = 0.2569 R2 = 0.8854 MRE=0.3242	LSV = 1.55E-6 R2 = 0.9700 MRE=0.0915	LSV = 3.1E-6 R2 = 0.9719 MRE=0.1771
Sulfur ppt/dissolution	r ($1.4x10^{-11}$ mol/s)	$2.1x10^{-11}$	LSV = 0.0156 R2 = 0.9508 MRE=0.2373	LSV = 2.4E-7 R2 = 0.9700 MRE=0.0915	LSV = 2.1E-7 R2 = 0.9719 MRE=0.1771

Table 2b. Sensitivity analysis results of the decreased 50 % variation of biokinetic parameters on each reaction.

Reaction	**Parameter**	**Average least-square value**			
	Baseline value	Decreased 50 %	Uranium concentration	Acetate concentration	Sulfate concentration
Sulfate bioreduction	q (10^{-8} mol/s/mg_{cells})	$1.5x10^{-8}$	LSV= 0.6459 R2 = 0.6414 MRE=0.5163	LSV = 0.1648 R2 = 0.8514 MRE=0.2344	LSV = 0.2358 R2 = 0.8296 MRE=0.3904
	k_D ($2x10^{-2}$ mol/L)	0.03	LSV= 0.3325 R2 = 0.8891 MRE=0.3452	LSV = 0.0632 R2 = 0.9854 MRE=0.0283	LSV = 0.0475 R2 = 0.9835 MRE=0.1281
	k_A ($2x10^{-2}$ mol/L)	0.03	LSV= 0.3474 R2 = 0.8794 MRE=0.3622	LSV = 0.0706 R2 = 0.9842 MRE=0.0295	LSV = 0.0476 R2 = 0.9815 MRE=0.1299
Fe(III) bioreduction	q (10^{-11} mol/s/mg_{cells})	$1.5x10^{-11}$	LSV= 0.0010 R2 = 0.9537 MRE=0.2334	LSV = 0.0004 R2 = 0.9699 MRE=0.0918	LSV = 0.0037 R2 = 0.9716 MRE=0.1788
	k_D ($2x10^{-2}$ mol/L)	0.03	LSV= 0.0018 R2 = 0.9542 MRE=0.2318	LSV = 0.0003 R2 = 0.9701 MRE=0.0913	LSV = 0.0037 R2 = 0.9721 MRE=0.1754
Sulfate bioreduction & Fe(III) bioreduction	Y (1600 mgc_{ells}/mol)	2400	LSV= 0.5270 R2 = 0.7435 MRE=0.4706	LSV = 0.0704 R2 = 0.9234 MRE=0.1616	LSV = 0.1049 R2 = 0.9190 MRE=0.2805
	b (10^{-8} 1/s)	$1.5x10^{-8}$	LSV= 0.0012 R2 = 0.9540 MRE=0.2323	LSV = 0.0002 R2 = 0.9701 MRE=0.0913	LSV = 0.0002 R2 = 0.9719 MRE=0.1768
U(VI) reduction	r ($8x10^{-11}$ mol/s)	$1.2x10^{-10}$	LSV = 0.5982 R2 = 0.6788 MRE=0.6683	LSV = 2.8E-5 R2 = 0.9700 MRE=0.0915	LSV = 0.0016 R2 = 0.9718 MRE=0.1776
	k_D ($4x10^{-2}$ mol/L)	0.06	LSV = 0.5062 R2 = 0.7874 MRE=0.4349	LSV = 2.39E-5 R2 = 0.9700 MRE=0.0915	LSV = 0.0011 R2 = 0.9719 MRE=0.1768
Fe(III) red. by HS-	r ($0.45x10^{-11}$ mol/s)	$6.75x10^{-12}$	LSV= 0.0191 R2 = 0.9484 MRE=0.2406	LSV = 7.55E-6 R2 = 0.9701 MRE=0.0915	LSV = 0.0010 R2 = 0.9718 MRE=0.1775
U(IV) reoxidation	r ($2x10^{-11}$ mol/s)	$3x10^{-11}$	LSV= 0.3282 R2 = 0.8727 MRE=0.3595	LSV = 1.33E-6 R2 = 0.9700 MRE=0.0915	LSV = 3.18E-6 R2 = 0.9719 MRE=0.1771
Sulfur ppt/dissolution	r ($1.4x10^{-11}$ mol/s)	$2.1x10^{-11}$	LSV= 0.0076 R2 = 0.9536 MRE=0.2331	LSV = 5.0E-7 R2 = 0.9700 MRE=0.0915	LSV = 5.3E-7 R2 = 0.9719 MRE=0.1771

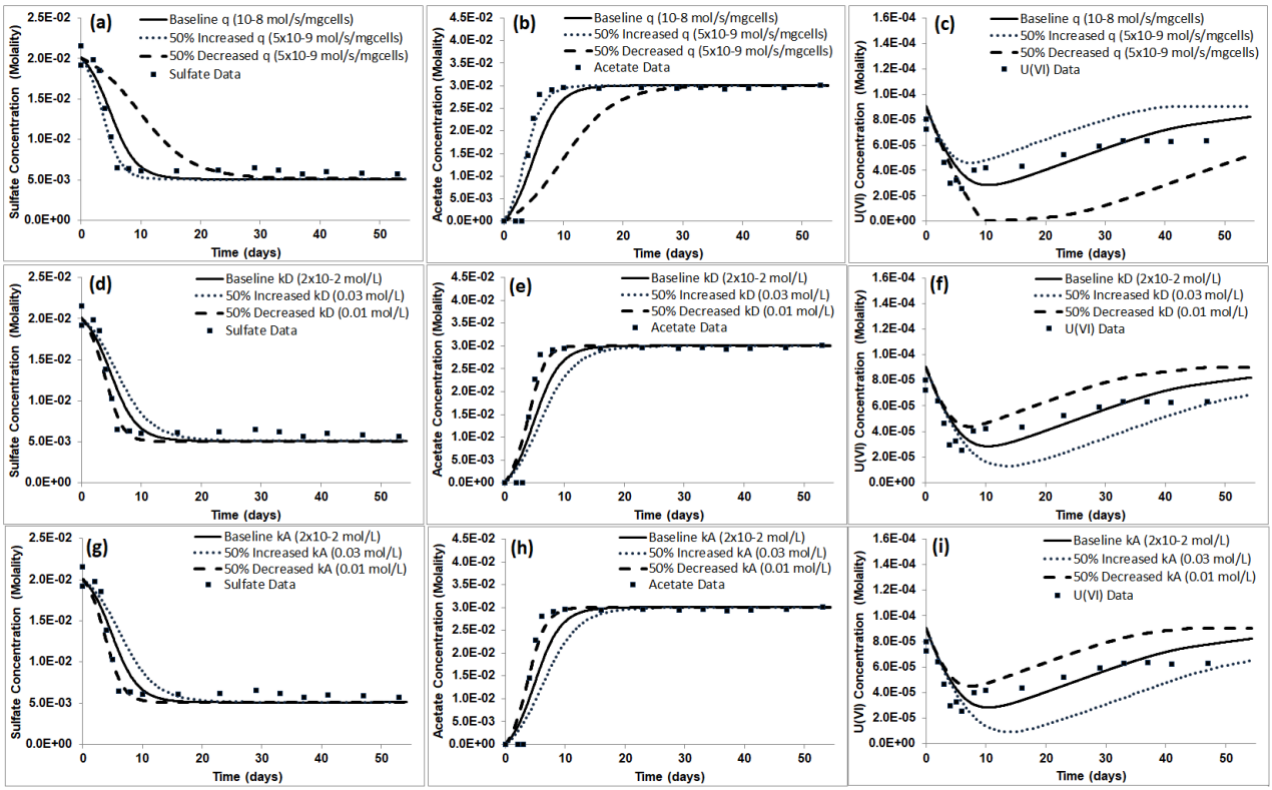

Figure 2. Impact of (a-c) maximum substrate utilization rate (q) on (a) sulfate, (b) acetate, (c) U(VI) concentration; impact of (d-f) half saturation constant for electron donor (k_D) on (d) sulfate, (e) acetate, (f) U(VI) concentration; impact of (g-i) half saturation constant for electron acceptor (k_A) on (g) sulfate, (h) acetate, (i) U(VI) concentration for the sulfate bioreduction reaction.

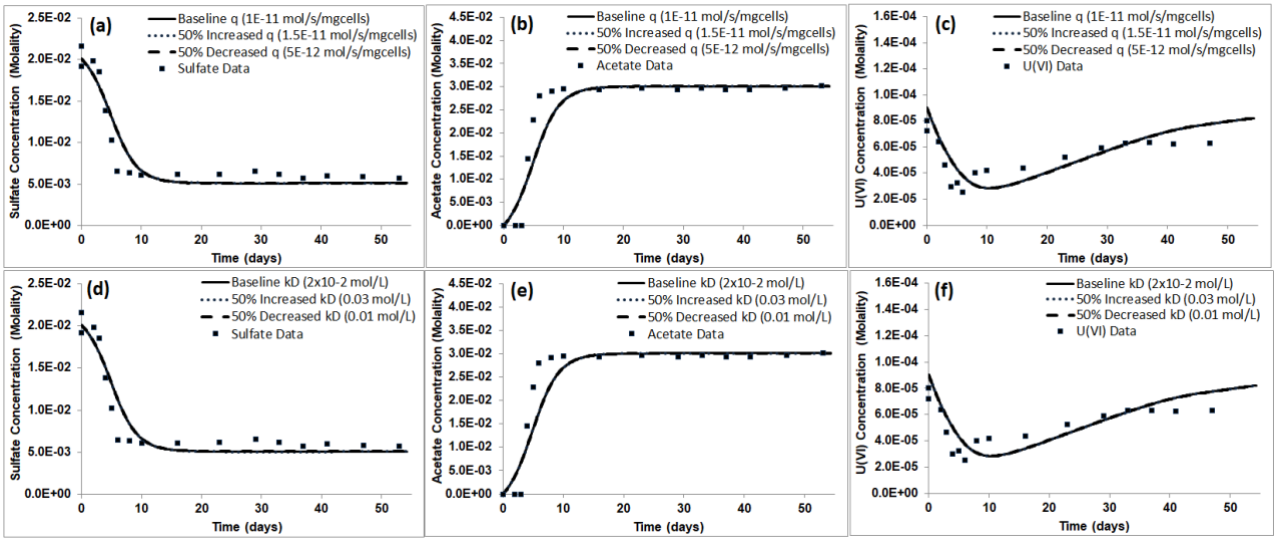

Figure 3. Impact of (a-c) maximum substrate utilization rate (q) on (a) sulfate, (b) acetate, (c) U(VI) concentration; impact of (d-f) half saturation constant for electron donor (k_D) on (d) sulfate, (e) acetate, (f) U(VI) concentration for the Fe(III) bioreduction reaction.

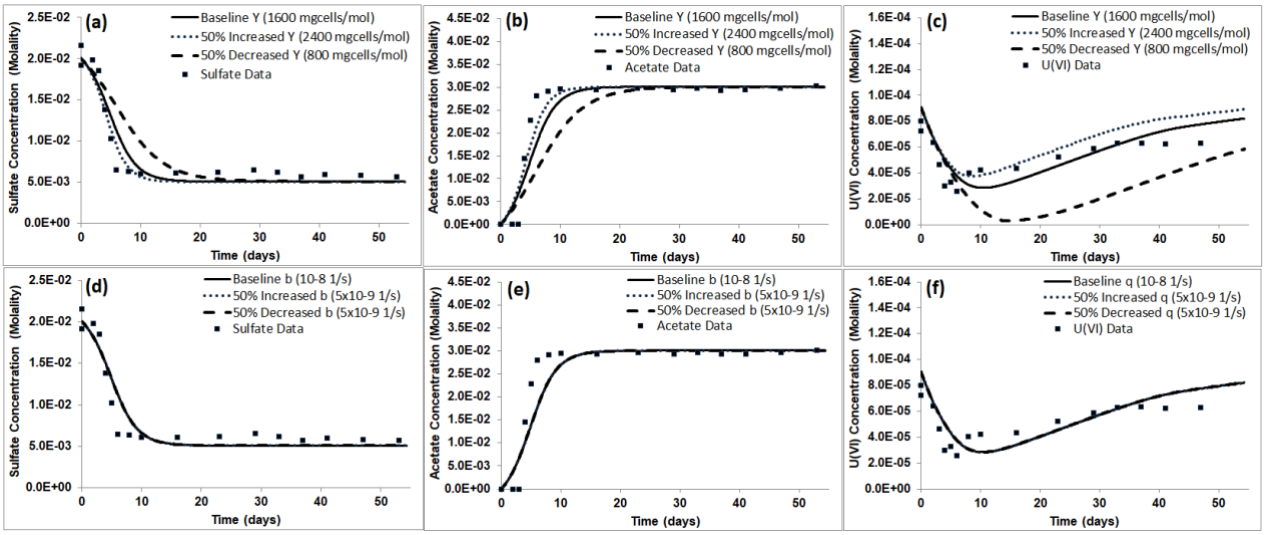

Figure 4. Impact of (a-c) microbial yield coefficient (*Y*) on (a) sulfate, (b) acetate, (c) U(VI) concentration; impact of (d-f) cell decay rate coefficient (*b*) on (d) sulfate, (e) acetate, (f) U(VI) concentration for the sulfate bioreduction & Fe(III) bioreduction reactions.

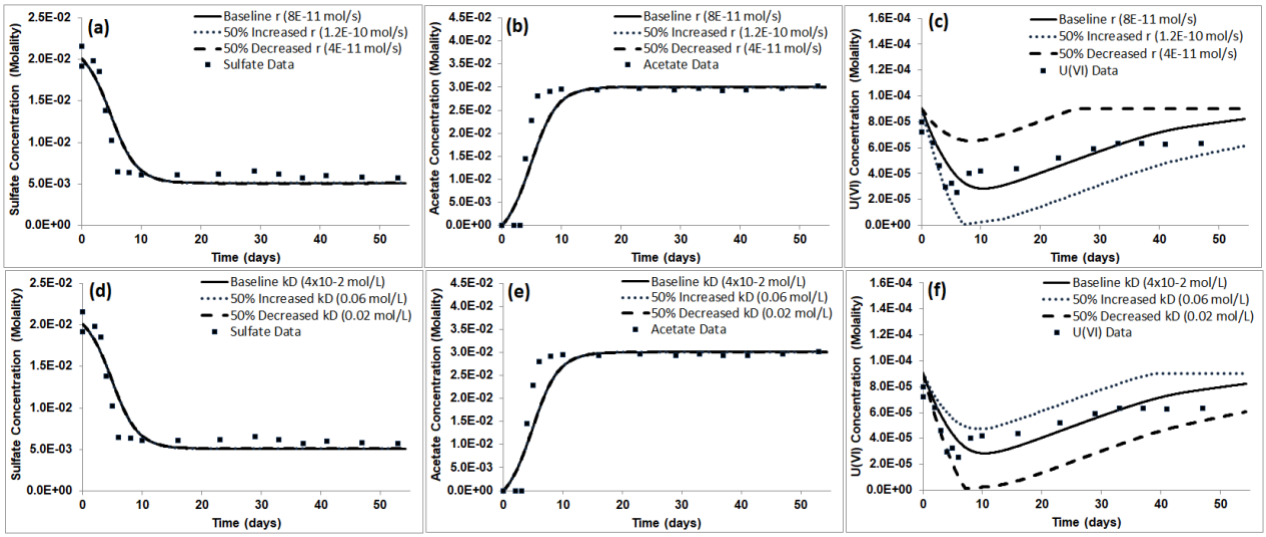

Figure 5. Impact of (a-c) rate constant (*r*) on (a) sulfate, (b) acetate, (c) U(VI) concentration; impact of (d-f) half saturation constant for electron donor (k_D) on (d) sulfate, (e) acetate, (f) U(VI) concentration for the U(VI) reduction reaction.

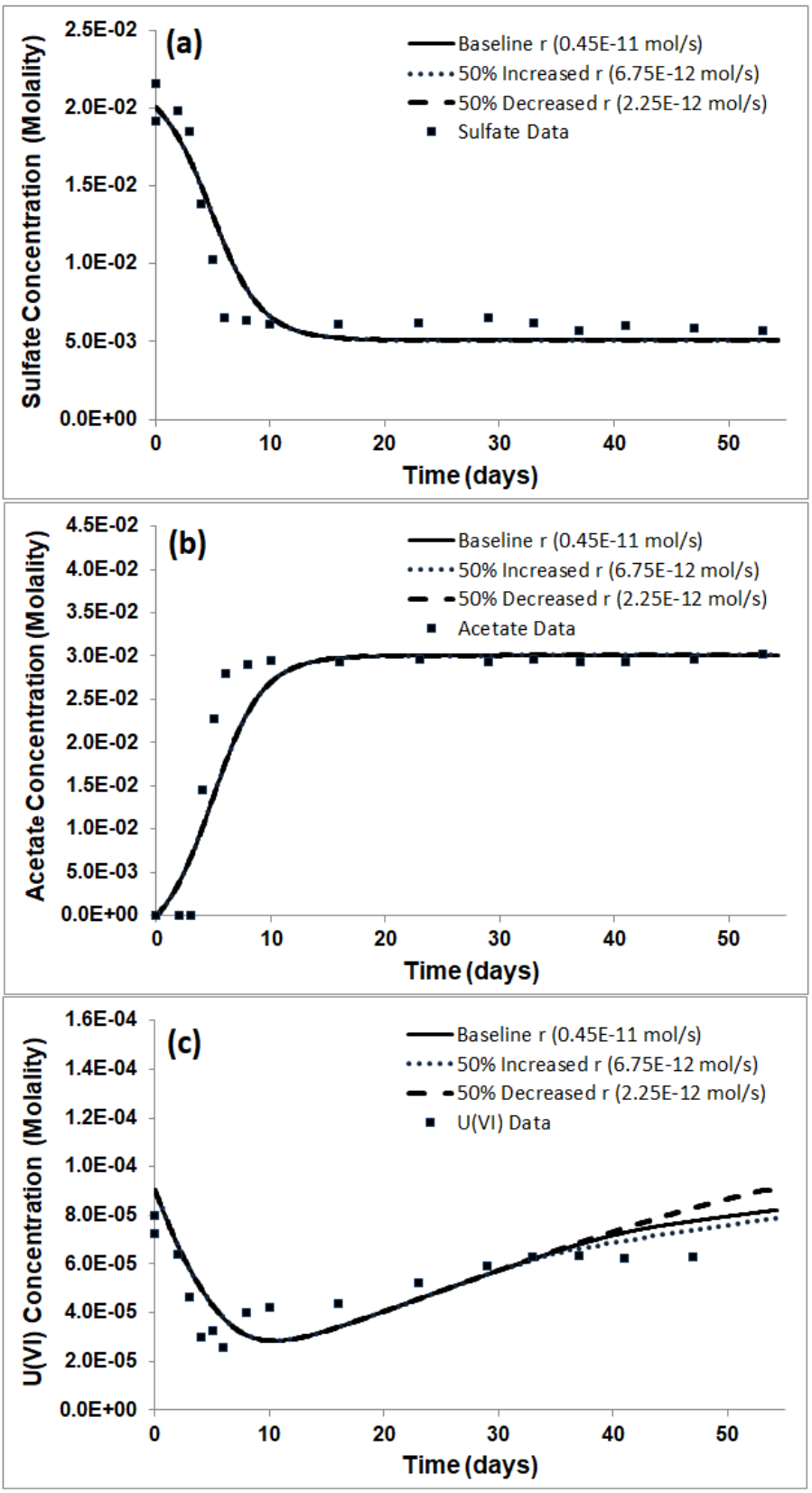

Figure 6. Impact of (a-c) rate constant (*r*) on (a) sulfate, (b) acetate, (c) U(VI) concentration for the Fe(III) reduction by HS^- reaction.

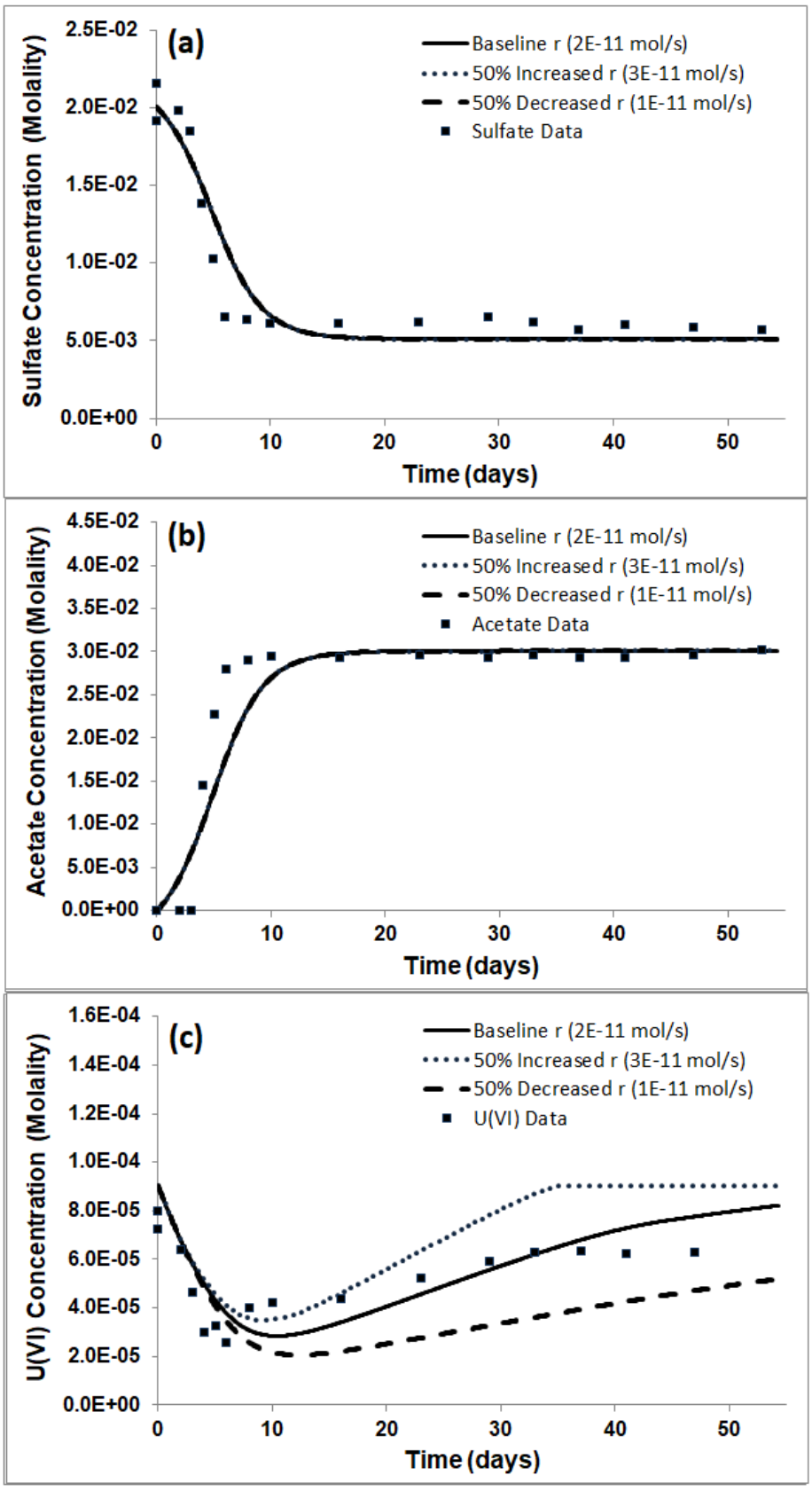

Figure 7. Impact of (a-c) rate constant (*r*) on (a) sulfate, (b) acetate, (c) U(VI) concentration for the U(IV) reoxidation reaction.

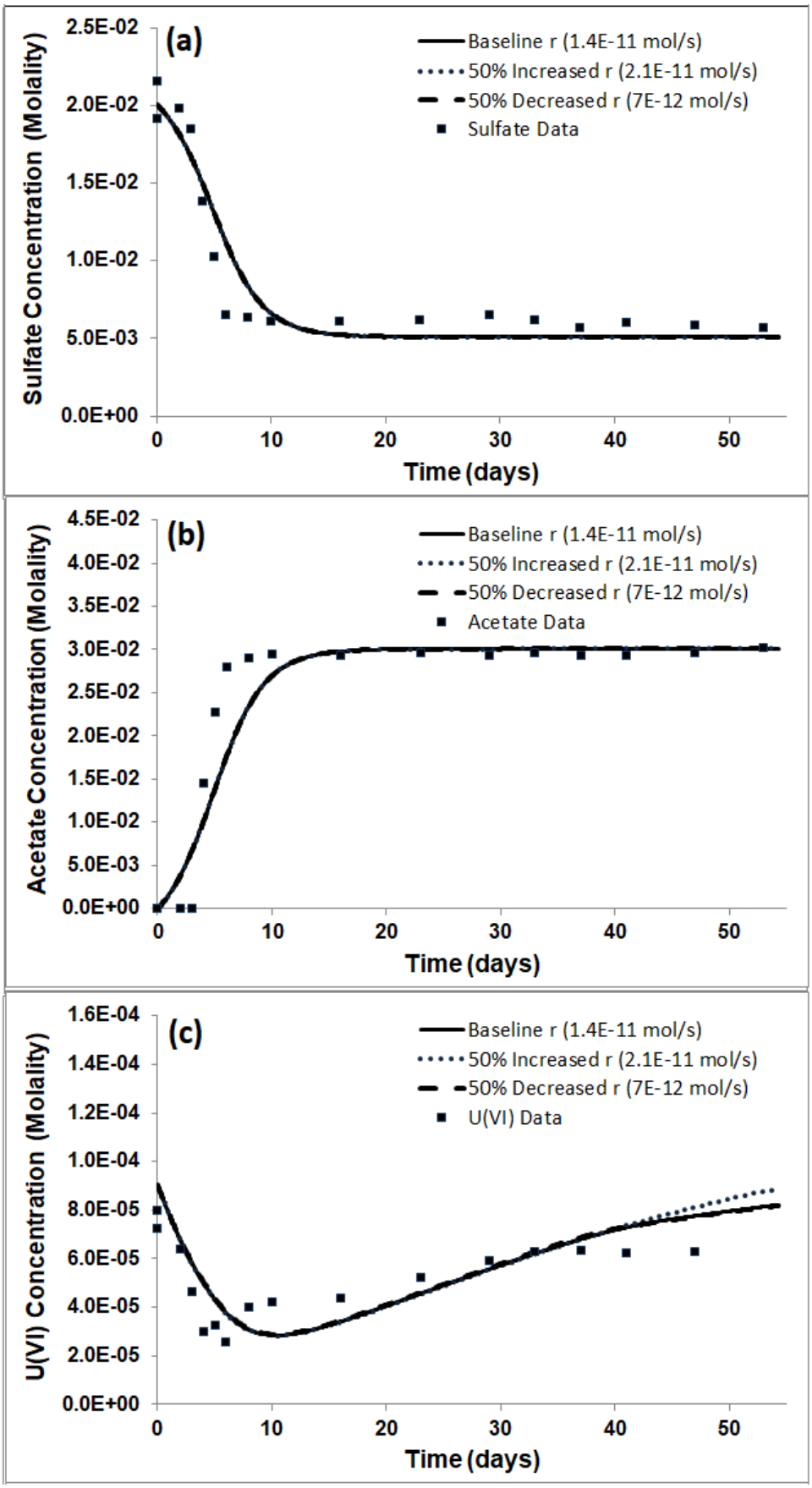

Figure 8. Impact of (a-c) rate constant (*r*) on (a) sulfate, (b) acetate, (c) U(VI) concentration for the Sulfur precipitation/dissolution reaction.

CONCLUSION

In this study, the impact of biokinetic parameters in modeling biological transformations of uranium are presented, based on the biogeochemical reaction network presented by Spycher et al. (2011) to model uranium bioreduction followed by reoxidation by Fe(III) (hydr)oxides. The key biogeochemical reactions include sulfate bioreduction and Fe(III) bioreduction reactions by lactate, U(VI) reduction to U(IV), Fe(III) reduction by HS^-, U(IV) reoxidation reaction to U(VI) and sulfur precipitation-dissolution reaction. The results of the sensitivity analysis show that the sulfate bioreduction was the most sensitive reaction to changes in the kinetic parameters; where the rate of maximum substrate utilization and yield coefficient had the most significant impact, and half-saturation constants had slightly more mild impact on model outcomes. U(VI) reduction and U(IV) reoxidation showed sensitivity only to the U(VI) concentration predictions with the changes in biokinetic parameters in these reactions. U(VI) concentrations were observed to be the most sensitive for the changes in biokinetics parameters among the simulated concentration predictions for all biogeochemical reactions. Although a delicate balance occurs in the system for competing rates of reactions for U(IV) reoxidation versus sulfide (HS^-) oxidation by Fe(III), Fe(III) reduction by HS^- and sulfur precipitation/dissolution reactions as well as Fe(III) bioreduction reactions did not show any sensitivity towards the changes in biokinetic parameters. The results presented in this study can help to improve process design conditions and removal efficiencies for uranium contaminated environments to be used for prediction purposes or for biodegradation models for uranium remediation.

Compliance with Ethical Standards

Peer-review

Externally peer-reviewed.

Declaration of Interests

The authors declared that for this research article, they have no actual, potential or perceived conflict of interest.

REFERENCES

Anderson, R. T., Vrionis, H. A., Ortiz-Bernad, I., Resch, C. T., Long, P. E., Dayvault, R., Karp, K., Marutzky, S., Metzler, D. R., Peacock, A., White, D. C., Lowe, M., & Lovley, D. R. (2003a). Stimulating the In Situ Activity of Geobacter Species to Remove Uranium from the Groundwater of a Uranium-Contaminated Aquifer. *Applied and Environmental Microbiology*, *69*(10), 5884–5891. https://doi.org/10.1128/AEM.69.10.5884-5891.2003

Baalbaki, Z., Torfs, E., Yargeau, V., & Vanrolleghem, P. A. (2017). Predicting the fate of micropollutants during wastewater treatment: Calibration and sensitivity analysis. *Science of the Total Environment*, *601*, 874-885.

Badriyha, B. N., Ravindran, V., Den, W., & Pirbazari, M. (2003). Bioadsorber efficiency, design, and performance forecasting for alachlor removal. *Water Research*, *37*(17), 4051-4072.

Chaudhuri, S. K., Lack, J. G., & Coates, J. D. (2001). Biogenic magnetite formation through anaerobic biooxidation of Fe (II). Applied and environmental microbiology, 67(6), 2844-2848.

China, M., & Kumar, S. (2004). Sensitivity analysis of biodegradation of soil applied pesticides using a simulation model. *Biochemical engineering journal*, *19*(2), 119-125.

Dastidar, A., & Wang, Y. T. (2009). Arsenite oxidation by batch cultures of Thiomonas arsenivorans strain b6. *Journal of Environmental Engineering*, *135*(8), 708-715.

Dastidar, A., & Wang, Y. T. (2012). Modeling arsenite oxidation by chemoautotrophic Thiomonas arsenivorans strain b6 in a packed-bed bioreactor. *Science of the total environment*, *432*, 113-121.

Den, W., & Pirbazari, M. (2002). Modeling and design of vapor-phase biofiltration for chlorinated volatile organic compounds. *AIChE journal*, *48*(9), 2084-2103.

Gihring, T. M., Zhang, G., Brandt, C. C., Brooks, S. C., Campbell, J. H., Carroll, S., Criddle, C. S., Green, S. J., Jardine, P., Kostka, J. E., Lowe, K., Mehlhorn, T. L., Overholt, W., Watson, D. B., Yang, Z., Wu, W. M., & Schadt, C. W. (2011). A limited microbial consortium is responsible for extended bioreduction of uranium in a contaminated aquifer. *Applied and Environmental Microbiology*, *77*(17), 5955–5965. https://doi.org/10.1128/AEM.00220-11

Gu, B., Wu, W. M., Ginder-Vogel, M. A., Yan, H., Fields, M. W., Zhou, J., Fendorf, S., Criddle, C. S., & Jardine, P. M. (2005). Bioreduction of uranium in a contaminated soil column. *Environmental Science and Technology*, *39*(13), 4841–4847. https://doi.org/10.1021/es050011y

Lens, P.N., Meulepas, R.J., Sampaio, R., Vallero, M. and Esposito, G. (2008). Bioprocess engineering of sulfate reduction for environmental technology. *In Microbial sulfur metabolism*. Springer Berlin Heidelberg. 285-295.

Lin, Y. H., & Wu, C. L. (2011). Sensitivity analysis of phenol degradation with sulfate reduction under anaerobic conditions. *Environmental Modeling & Assessment*, *16*, 213-225.

Malaguerra, F., Chambon, J. C., Bjerg, P. L., Scheutz, C., & Binning, P. J. (2011). Development and sensitivity analysis of a fully kinetic model of sequential reductive dechlorination in groundwater. *Environmental science & technology*, *45*(19), 8395-8402.

Moriasi, D. N., Gitau, M. W., Pai, N., & Daggupati, P. (2015). Hydrologic and water quality models: Performance measures and evaluation criteria. *Transactions of the ASABE*, *58*(6), 1763-1785.

Neumann, M. B. (2012). Comparison of sensitivity analysis methods for pollutant degradation modelling: A case study from drinking water treatment. *Science of the total environment*, *433*, 530-537.

Parkhurst, D. L., & Appelo, C. A. J. (2013). Description of input and examples for PHREEQC version 3—a computer program for speciation, batch-reaction, one-dimensional transport, and inverse geochemical calculations. *US geological survey techniques and methods*, *6*(A43), 497.

Pontes, R. F., Moraes, J. E., Machulek Jr, A., & Pinto, J. M. (2010). A mechanistic kinetic model for phenol degradation by the Fenton process. *Journal of hazardous materials*, *176*(1-3), 402-413.

Riefler, R. G., Ahlfeld, D. P., & Smets, B. F. (1998). Respirometric assay for biofilm kinetics estimation: parameter identifiability and retrievability. *Biotechnology and bioengineering*, *57*(1), 35-45.

Renshaw, J. C., Butchins, L. J. C., Livens, F. R., May, I., Charnock, J. M., & Lloyd, J. R. (2005a). Bioreduction of uranium: Environmental implications of a pentavalent intermediate. *Environmental Science and Technology*, *39*(15), 5657–5660. https://doi.org/10.1021/es048232b

Sani, R. K., Peyton, B. M., Amonette, J. E., & Geesey, G. G. (2004). Reduction of uranium (VI) under sulfate-reducing conditions in the presence of Fe (III)-(hydr) oxides. *Geochimica et Cosmochimica Acta*, *68*(12), 2639-2648.

Scarlat, E., Zapodeanu, D., & Ioan, C. M. (2014). Comparing Smoothing Technique Efficiency in Small Time Series Datasets after a Structural Break in Mean. In *Recent Developments in Computational Collective Intelligence* (pp. 145-153). Springer International Publishing.

Seyfi, H., Shafiei, S., Dehghanzadeh, R., & Amirabedi, P. (2021). Mathematical Modeling and Parameters Optimization of the Degradation of Acrylonitrile in Biofilters. *Iranian Journal of Chemical Engineering (IJChE)*, *18*(3), 3-15.

Spycher, N. F., Issarangkun, M., Stewart, B. D., Şengör, S. S., Belding, E., Ginn, T. R., ... & Sani, R. K. (2011). Biogenic uraninite precipitation and its reoxidation by iron (III)(hydr) oxides: A reaction modeling approach. *Geochimica et Cosmochimica Acta*, *75*(16), 4426-4440.

Şengör, S. S., Mayer, K. U., Greskowiak, J., Wanner, C., Su, D., & Prommer, H. (2015). A reactive transport benchmark on modeling biogenic uraninite re-oxidation by Fe (III)-(hydr) oxides. *Computational geosciences*, *19*, 569-583.

Tokunaga, T. K., Wan, J., Kim, Y., Daly, R. A., Brodie, E. L., Hazen, T. C., Herman, D., & Firestone, M.K. (2008). Influences of organic carbon supply rate on uranium bioreduction in initially oxidizing, contaminated sediment. *Environmental Science and Technology*, *42*(23), 8901–8907. https://doi.org/10.1021/es8019947

Vázquez-Rodríguez, G., Youssef, C. B., & Waissma-Vilanova, J. (2006). Two-step modeling of the biodegradation of phenol by an acclimated activated sludge. *Chemical Engineering Journal*, *117*(3), 245-252.

Walpole, R. E., Myers, R. H., Myers, S. L., & Ye, K. (1993). *Probability and statistics for engineers and scientists* (Vol. 5, pp. 326-332). New York: Macmillan.

Wilkins, M. J., Livens, F. R., Vaughan, D. J., & Lloyd, J. R. (2006). The impact of Fe(III)-reducing bacteria on uranium mobility. *Biogeochemistry*, *78*(2), 125–150. https://doi.org/10.1007/s10533-005-3655-z

Wufuer, R., Wei, Y., Lin, Q., Wang, H., Song, W., Liu, W., ... & Gadd, G. M. (2017). Uranium bioreduction and biomineralization. *Advances in applied microbiology*, *101*, 137-168.

Yabusaki, S. B., Fang, Y., Williams, K. H., Murray, C. J., Ward, A. L., Dayvault, R. D., ... & Long, P. E. (2011). Variably saturated flow and multicomponent biogeochemical reactive transport modeling of a uranium bioremediation field experiment. *Journal of contaminant hydrology*, *126*(3-4), 271-290.

Zhou, X. H., Liu, J., Song, H. M., Qiu, Y. Q., & Shi, H. C. (2012). Estimation of heterotrophic biokinetic parameters in wastewater biofilms from oxygen concentration profiles by microelectrode. *Environmental Engineering Science*, *29*(6), 466-471